**NURETH14-177** 

# STUDY ON TEMPERATURE FLUCTUATION PHENPMENON IN PRESSURIZER SPRAY PIPE OF PRESSURIZED WATER REACTOR

# Hideki TAMURA<sup>1</sup>, Yusuke OZAKI<sup>1</sup>, Nobuyuki TAKENAKA<sup>1</sup>, Koji MIYOSHI<sup>2</sup> and Akira NAKAMURA<sup>2</sup>

<sup>1</sup> Department of Mechanical Engineering, Kobe University, Hyogo, Japan <sup>2</sup> Institute of Nuclear Safety System Incorporated, Fukui, Japan

#### **Abstract**

Damage of a pressurizer spray piping in a PWR plant is potentially considered from a safety point of views. Gas-liquid interface is formed in the pressurizer spray pipe of the PWR under a rated power operating condition. Temperature fluctuation may occur if the interface may move periodically. Measurement of inner wall and fluid temperature in the test section simulating the real pressurizer spray pipe was conducted to study mechanism of the temperature fluctuation phenomena. The temperature fluctuations were observed. Visualization experiment was conducted to understand the flow phenomena. It was estimated that Kelvin-Helmholtz instability occurred in the liquid layer in a horizontal pipe in the spray piping.

#### 1. Introduction

Pipes of an industrial plant, including the nuclear plant, may be damaged due to the thermal fatigue by the temperature fluctuation. The damages of the branching pipe due to the thermal fatigue have been reported. The damage of the pressurizer spray piping is potentially considered from a safety point of views. Schematic figure of the pressurized spray pipe is shown in Figure 1. There are low-temperature water (about 290 degree Celsius), high-temperature vapor (about 345 degree Celsius), and non-condensable gas, hydrogen, which is one of products of water radiolytic, in the pressurizer spray pipe. Counter-current water and vapor flow in the pipe. Gas-liquid interface is formed in the pressurizer spray pipe of the pressurized water reactor when the flow rate is small under a rated power operating condition. The pressurizer spray pipe may be damaged due to the thermal fatigue by the temperature fluctuation if the interface may move periodically. Measurement of inner wall and fluid temperature in the test section simulating the real pressurizer spray pipe was carried out to study mechanism of the temperature fluctuation phenomena. Visualization experiment was carried out at the horizontal part of the spray pipe to understand the flow phenomena in the pipe.

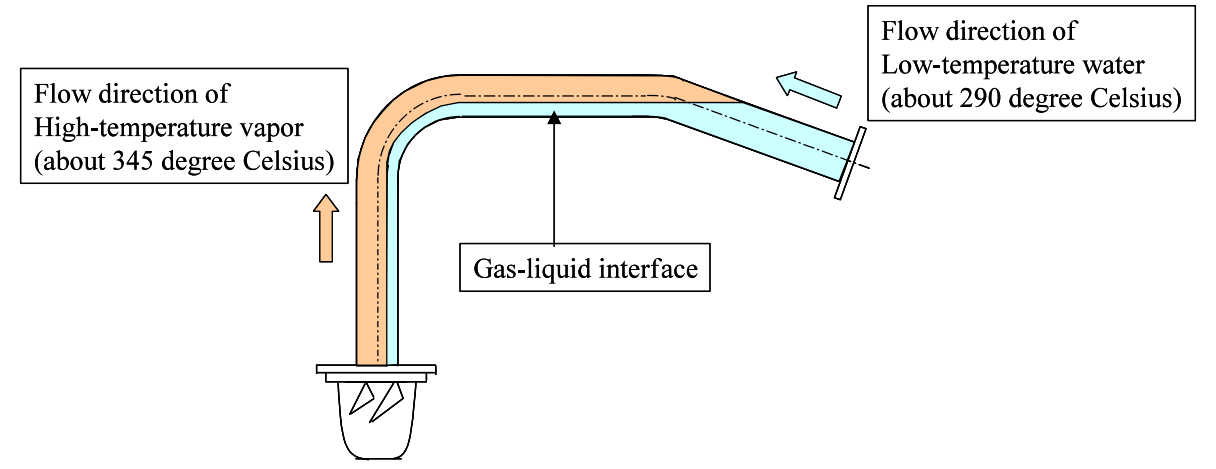


Figure 1 Schematic figure of the pressurized spray pipe

### 2. Experimental apparatus and conditions

An experimental loop was constructed to conduct the two-phase flow experiments with steam and water for the gas and liquid phase, respectively.

The outline of the experimental loop is shown in Figure 2. The working fluid was deaerated water, which was boiled in an external tank for degas and supplied to the loop. The flow direction of water is indicated by the arrow in Figure 2. The entire loop was maintained at atmospheric pressure. Water and steam temperature were kept at 60 and 100 degree Celsius respectively. The water was heated in the tank simulating the pressurizer was cooled down by the heat exchanger, pumped to the test section and returned to the tank again. Flow rate was measured by the flow meter placed downstream of the bypass. The temperatures were measured for 90 minutes at the bypass flow rate,  $0.46\text{m}^3/\text{h}$ , of the PWR plant.

In addition, the air tank was equipped at the top of the tank simulating pressurizer and the air was injected evaluate effects of the non-condensable gas on the flow pattern and the temperature fluctuation. The air is non-condensable gas as well as the hydrogen gas and was heated to 100 degree Celsius to keep the vapor temperature after the injection. Mass of the injected air was measured by pressure difference in the air tank before and after the injection. Dissolved oxygen concentration was measured by the dissolved oxygen meter.

Configuration of the test section is shown in the Figure 3 with the location of thermocouples. The test section consists of a full-scale mock-up of the spray pipe and the nozzle, which simulate the spray pipe in a real PWR plant. The nominal size of the test section was 4B • Sch.160. The inner diameter and the wall thickness were 87.3mm and 13.5mm respectively. Five cross sections labeled A  $\sim$  C, E, and P are shown by the capital letters with a circle in Figure 3. Two lines on the outside of the test section each labeled F and G shown in the capital letter with a circle in Figure 3. Stainless steel sheathed thermocouples 1mm in diameter were installed on the inner surface to measure the inner wall temperature fluctuation. The thermocouples of 0.5mm in wire diameter were banded together in a rod and inserted in the pipe to measure fluid temperature fluctuation at the section A  $\sim$  C and E. Four sheathed thermocouples were installed with 45 degree angle increment at the cross section A  $\sim$  C and E. Five thermocouples were lined in 20mm internal at the cross section A  $\sim$  C. Ten thermocouples were lined in 9mm interval at the cross section E.

The section P was replaced from a stainless steel pipe to a transparent polycarbonate resin pipe for the visualization experiment. The sizes of the polycarbonate pipe were the same as the stainless steel pipe. The fluid temperature distributions were measured at the cross section P under the visualization condition. The fifteen thermocouples of 0.5mm in diameter were banded together in a rod with 2mm increment and inserted in the pipe to measure fluid temperature distribution around liquid-vapor interface at the cross section P.

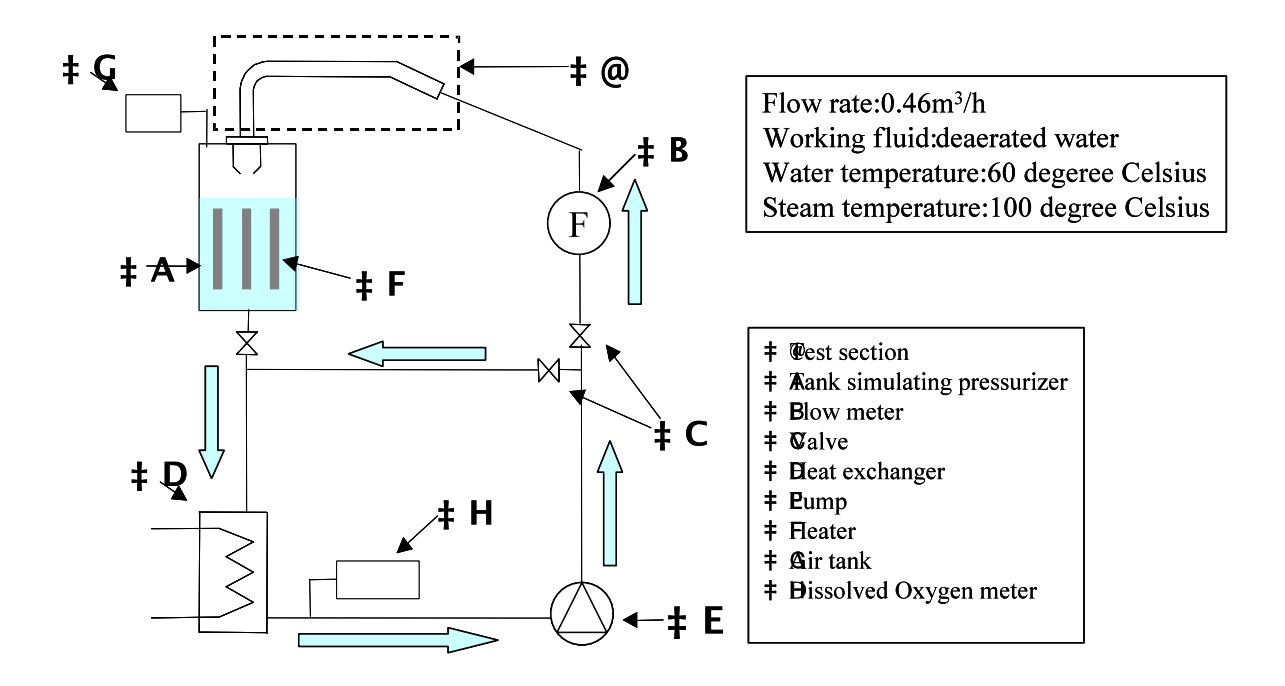


Figure 2 Schematic diagram of the test loop

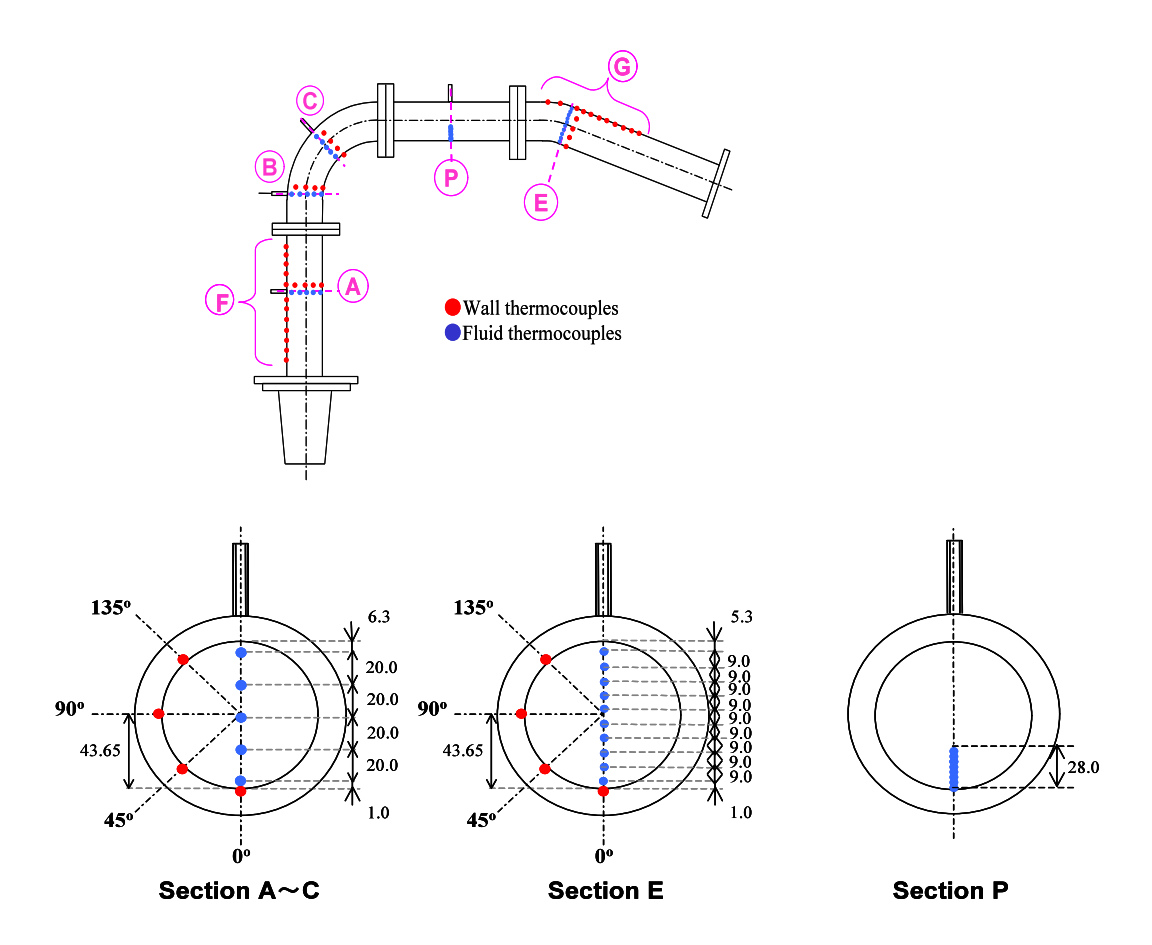


Figure 3 Positions of thermoelectric couples

# 3. Experimental results and discussion

#### 3.1 Water and wall temperature fluctuations

Experiments with the stainless steel pipe, i.e., without visualization were conducted at first. Notable temperature fluctuations were observed at the section E in Figure 3. Time histories of temperature where notable fluctuations were observed are shown in Figure 4. The maximum temperature fluctuation of about 7 Kelvin was observed at 90 degree at the cross section E. The fluctuation periods were in wide ranges from 10s to 200s.

A time history of the temperature fluctuation at 90 degree at the cross section E before and after the air injection process is shown in Figure 5. It is shown that the fluctuation stops just after the air, the non-condensable gas, is injected.



Figure 4 Recorder chart of the wall temperature fluctuation in vapor and water system at section E

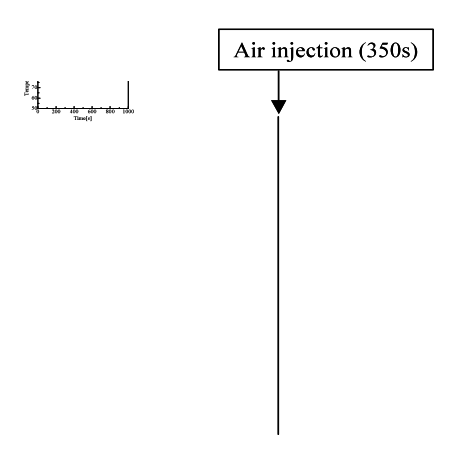


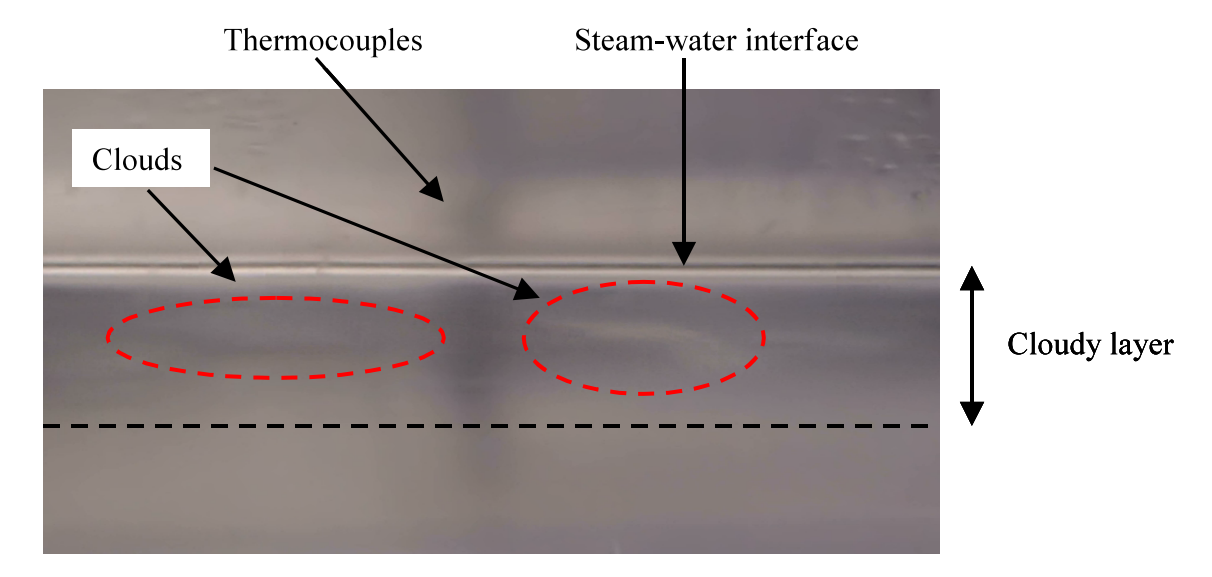
Figure 5 Recorder chart of the wall temperature fluctuation before and after the air injection

## 3.2 Visualization and temperature distributions at the visualization test section

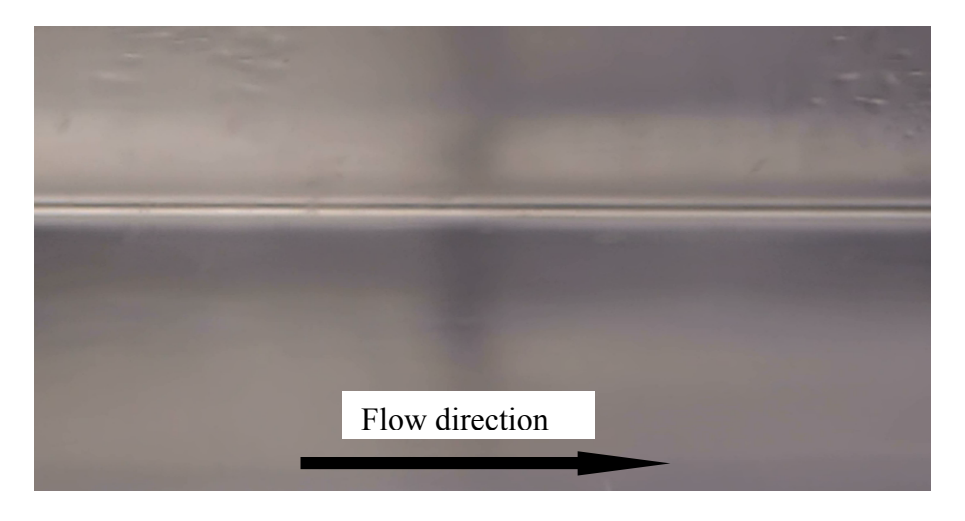
Visualization experiments were conducted to investigate the temperature fluctuation phenomena as shown in Figures 4 and 5. Visualization results with and without the non-condensable gas at the test section are shown in Figure 6. The movement of the gas-liquid

interface was not observed in both conditions. However, a cloudy layer below the gas-liquid interface can be seen in the experiment without the non-condensable gas. The clouds in Figure 6 flowed to the flow direction periodically. The width of the layer was about 10mm. It is estimated that the layer looks cloudy due to the shadowgraph effects by the water density distribution due to the temperature fluctuations.

The time history of temperature fluctuations on the air injection process at the section P in Figure 3 is shown in Figure 7. It is shown that large fluid temperature fluctuations are observed before the air injection at time 130s and then the fluctuations were reduced just after the air injection.



Before the air injection



After the air injection

Figure 6 Visualization near the gas-liquid interface before and after the air injection

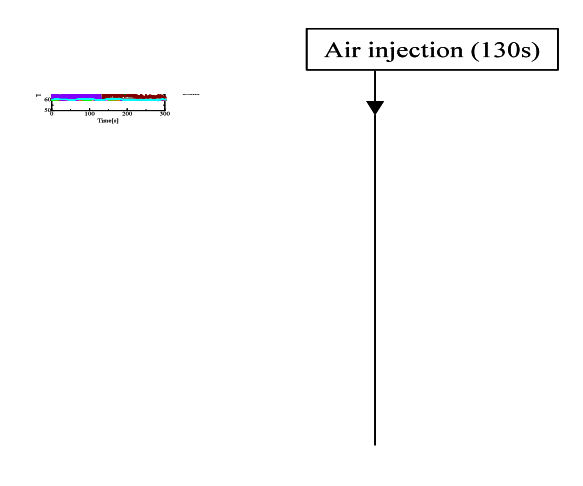


Figure 7 Recorder chart of the temperature fluctuation on the air injection process at section P

The temperature distributions at the cross section P with and without the non-condensable gas are shown in Figures 8 and 9. Temperature distributions time-averaged for 30 minutes are plotted. The length of bar at each measurement point indicates the maximum and minimum temperature fluctuations during the measurement. The horizontal axis is the distance from the pipe bottom. The vertical line in these figures indicates the steam-water interface. The temperature increased from 60 to 100 degree Celsius with increasing the distance from the pipe bottom. The notable temperature fluctuation was observed in the range of 14mm~24mm from the pipe bottom before the air injection. The maximum fluctuation was about 35 Kelvin at 14mm from the pipe bottom. The results of the measured temperature distributions and the visualization indicated that the large temperature fluctuations occurred in the cloudy layer below the steam-water interface.

It was also shown that the non-condensable gas reduced the liquid temperature fluctuations by comparing Figures 8 and 9. The mass of the injected air was equivalent to 0.27ppm if all air dissolved into water. This concentration was much smaller than the hydrogen concentration in the PWR water. Therefore, it is expected that similar liquid temperature fluctuations may not occur in the spray pipe of the operating PWR.

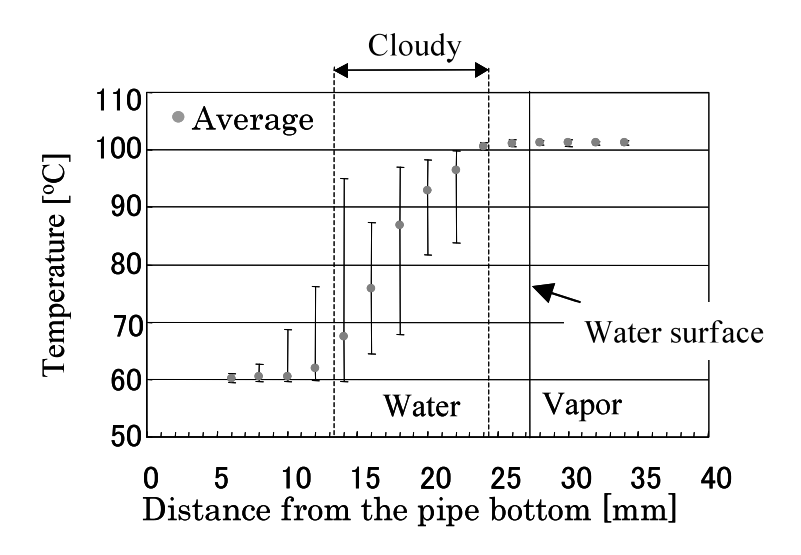


Figure 8 Temperature distribution at P-section before the air injection

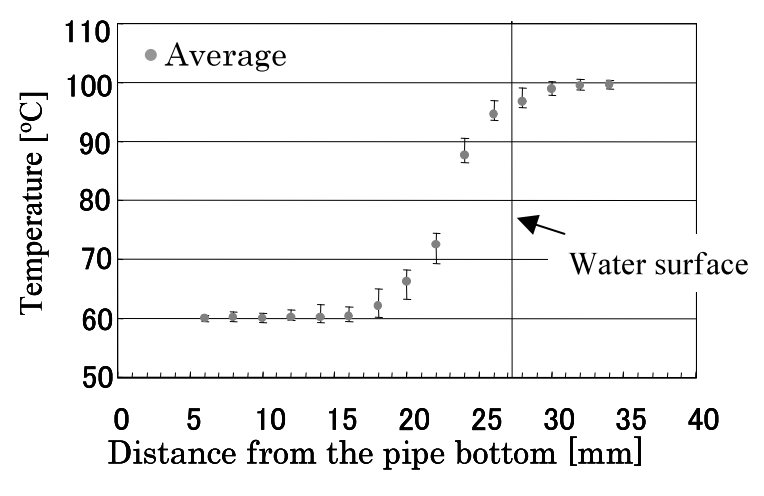


Figure 9 Temperature distribution at P-section after the air injection

It is well known that waves appear at an interface of two fluids the velocities and the densities of which are different. This phenomena is generally called Kelvin-Helmholtz instability when the density of the upper fluid is smaller than that of the lower one. The instability occurs at the interface when the difference between the velocities of the two layers reaches a certain value.

Figure 10 shows an illustration of the Kelvin-Helmholtz instabilities between high and low temperature liquid layer below the steam-water interface.

The stability limitation of the velocity difference is given by Equation (1).

$$\left|u_{L1} - u_{L2}\right| = \sqrt{\frac{\rho_{L2}I_{L2} + \rho_{L1}I_{L1}}{\rho_{L2}I_{L2} \cdot \rho_{L1}I_{L1}}} \left[ \left(\rho_{L2} - \rho_{L1}\right) \frac{\lambda g}{2\pi} \right]$$
(1)

, where  $I_{L1}$ = $coth2 \pi h_{L1}/\lambda$   $I_{L2}$ = $coth2 \pi h_{L2}/\lambda$ 

The velocity distribution in the liquid phase has not been measured in the present paper. It is estimated that the steam condensation of countercurrent flows from the tank may decrease the velocity of the steam-water interface. Kelvin-Helmholtz instability may occur at the interface between the low density, low velocity upper layer and the high density, high velocity lower layer and caused the notable temperature fluctuation below the steam-water interface as shown in Figure 7.

Condensation heat transfer rate, Q [W] and mass transfer rate, M [kg/s] were calculated by the liquid temperature distributions shown in Figures 8 and 9. Q was calculated by enthalpy difference of liquid using the following Equation (2).

$$Q = \rho C_p U \sum_i \Delta T_i I_i \delta - Q_c \tag{2}$$

$$q = Q/S \quad , m = M/S \tag{3}$$

, where  $\rho$  is the liquid density,  $C_p$  is the specific heat, U is the averaged liquid velocity,  $\Delta T$  is the difference between the inlet temperature and the measured temperature, l is the horizontal length at the cross section,  $\delta$  is the interval length of the measured points, and i is the index of the measured points.  $Q_c$  is the heat transfer rate by convection calculated by the Dittus Boelter's equation. M is calculated by  $Q_c$  and the latent heat of evaporation. S is the area of the steam-water interface from the inlet to the points where the liquid temperature is measured. It was assumed that the liquid flow velocity was uniform and the liquid temperature was uniform at the horizontal area at the measured points.

Table 1 shows the heat flux q [kW/m²] and the mass flux m [kg/m²·s] calculated before and after the air injection. It was shown that the material flow rate was less than half after the air injection. It is considered that the non-condensable gas suppressed the steam condensation and the heat transfer. It seems that the shear stress in the water interface might decrease and the velocity of upper layer might increase after the air injection. Therefore, the instability could not occur by the reduction of the velocity below water interface after the air injection. We plan to measure the velocity distribution in liquid phase before and after the air injection in future to verify this assumption.



Figure 10 An interfacial wave between high temperature layer and low temperature layer

Table 1 Numerical values of q, m

	$q[\mathrm{kW/m^2}]$	$m[kg/m^2 \cdot s]$
Before the air injection	$3.0 \times 10^{2}$	1.31×10 <sup>-1</sup>
After the air injection	$1.3 \times 10^2$	5.5×10 <sup>-2</sup>

#### 4. Conclusion

The steam-water experiments with the full-scale stainless steel mock-up simulating a real PWR plant were conducted at the bypass flow rate. The maximum wall temperature fluctuations about 7 Kelvin were observed. The causes of the wall temperature fluctuations in the pressurizer spray piping by visualization experiments for a steam-water two-phase flow are discussed in the paper. Also, the effect of non-condensable gas on the wall temperature fluctuations is discussed by those visualization tests. The following conclusions were obtained.

- 1. The wall temperature fluctuations were not caused by the movement of the water surface, but were caused by the liquid temperature fluctuations in the water layer below the steam-water interface.
- 2. Non-condensable gas reduced the liquid temperature fluctuations in the layer below the steam-water interface
- 3. It was inferred that the liquid temperature fluctuations in the cloudy layer were caused by the Kelvin-Helmholtz instabilities in the water layer due to the condensation mass transfer.